Engineering Science and Technology, an International Journal 22 (2019) 610–617

HOSTED BY

Contents lists available at ScienceDirect

Engineering Science and Technology, an International Journal

journal homepage: www.elsevier.com/locate/jestch

Full Length Article

Thermal analysis of lithium ion battery-equipped smartphone explosions

Kyung Mo Kim, Yeong Shin Jeong, In Cheol Bang *

Department of Nuclear Engineering, Ulsan National Institute of Science and Technology (UNIST), 50 UNIST-gil, Ulju-gun, Ulsan 44919, Republic of Korea

ARTICLE INFO

Article history:
Received 6 June 2018
Revised 13 December 2018
Accepted 18 December 2018
Available online 26 December 2018

Keywords:
Smartphone
Thermal analysis
Cooling
Lithium ion battery
Heat pipe

ABSTRACT

Thermal management of mobile electronics has been carried out because performance of the application processor has increased and power dissipation in miniaturized devices is proportional to its functionalities. There have been various studies on thermal analyses related to mobile electronics with the objectives of improving analysis methodologies and cooling strategies to guarantee device safety. Despite these efforts, failure to control thermal energy, especially in smartphones, has resulted in explosions, because thermal behaviors in the device under various operating conditions have not been sufficiently conducted. Therefore, several scenarios that caused the failure in thermal management of smartphone was analyzed to provide improved insight into thermal design deducing the parameters, that affect the thermal management of device. Overcurrent in battery due to malfunction of battery management system or immoderate addition of functionalities to the application processor are considered as reliable causes leading to the recent thermal runaways and explosions. From the analyses, it was also confirmed that the heat generation of the battery, which have not been considered importantly in previous literature, has significant effect on thermal management, and heat spreading could be suppressed according to arrangement of AP and battery. The heat pipe, which is utilized as a cooling device in mobile electronics, was also included in the thermal analyses. Although the heat pipes have been expected to improve the thermal management in mobile electronics, it showed limited heat transfer capacity due to its operating conditions and miniaturization. The demonstrated results of our analysis warn against vulnerabilities of smartphones in terms of safety in design.

1. Introduction

It is necessary to maintain the operating temperatures within acceptable limits for proper operation of the components of mobile electronic devices [1,2]. Heat management is a typical bottleneck in future development of smartphones because the functionalities and required levels of power dissipation are increasing while sizes of the devices are being miniaturized. If overheating occurs in the device due to failure of thermal management, the performances of components will be degraded. This may be accompanied by thermal runaway and explosion of battery, which is a threat to user safety and may result in fatalities. Recent examples of these are the explosions of smartphones. The thermal behaviors of smartphones have been analyzed by numerical simulations [1–5] and experiments [6–18] for optimizing the arrangement of components and construction of circuits with consideration about heat transport media such as thermal interface materials, heat sinks, and metal brackets. In the aspect of cooling strategies, the applicability of fan cooling in smartphones was confirmed by observing the relations between pressure drop, temperature drop, and flow velocities as seen in blockage structures simulating the layout of chipsets [6–9]. However, active cooling based on a fan has side effects such as additional power consumption, noise, and difficulties in waterproofing and dustproofing. Phase change materials (PCMs) have been studied for their use as heat sinks in application processors (AP) owing to insufficient presence of heat sinks in the present structures of the devices [10–13]. Although they can achieve better heat transport in short-term cooling compared to heat transport media installed in current devices, their performances might be lowered when the PCMs completely change to a liquid phase. A candidate for dealing with heat generation in electronics is the heat pipe. Heat pipe is a passive heat transport device installed between the hotter and cooler sections by storing working fluid in liquid phase inside a metal container and placing wick structures in it. The working fluid evaporates at the hotter section with absorption of heat. The generated vapor turns into

* Corresponding author.
E-mail address: icbang@unist.ac.kr (I.C. Bang).
Peer review under responsibility of Karabuk University.

https://doi.org/10.1016/j.jestch.2018.12.008
2215-0986/

Nomenclature

h	heat transfer coefficient [W/m^2 K]
I	current [A]
k	thermal conductivity [W/m K]
n	unit normal vector from surface [m]
Q	heat [W]
r	radius [m]
S	internal heat source [W/m^3]
s	surface area [m^2]
T	temperature [°C]
t	time [s]
U	voltage [V]
V	volume [m^3]
x	space coordinates

Greek symbols

ρ	volumetric heat capacity [J/m^3 K]

Subscript

ocv	open circuit voltage
reac	reaction
sk	sink
soc	state of charge

liquid state at the colder section. The liquid is then transported to the hotter section using capillary pumping pressure induced by the wick structures. Various types of heat pipes were designed and tested for their applicability in miniaturized electronic devices [14–20]. The heat pipes spread the heat generated in the AP to colder parts to decrease the AP temperature. Many smartphones used heat pipes for their thermal management systems. The heat spreading ability of the heat pipes is expected to be superior compared to existing conductors. Nevertheless, temperature difference between the hotter and colder sections will be reduced (thermal flattening) in long-term operation if a constant heat sink temperature is not assured. Because performance of the heat pipe is determined by the temperature difference between hotter and cooler sections, the heat transfer rate of the heat pipe will decrease eventually. Recent heat management strategies using heat pipes cannot be the ultimate solution for high-performance smartphones. Additionally, several elements of risk threaten the integrity of smartphones. For example, software that controls the current and voltage in the circuit can fail and there are no provisions against such failures. Hence, causes or risk factors that resulted in explosions of smartphone must be identified to prevent future accidents. Here, we have postulated the accident scenarios that can lead to thermal runaway and explosion of the battery in Galaxy Note 7 as follows. First, AP alone is subjected to the overcurrent. Next, high-power consuming operations of the chipset last for a long time causing overcurrent in both the battery and AP. The existing literatures related to thermal analysis of mobile electronics did not consider the heat generation of batteries. Nonetheless, lithium-ion batteries (LIB) generate heat during operation [21]. Self-heating of battery can be a crucial factor in a confined space because when the battery temperature increases to a certain point, it will induce thermal runaway. In thermal runaway, energy stored in the battery is converted to thermal energy rather than electrical energy, which eventually causes combustion of the constituents [22,23]. Therefore, heat generation in the battery was regarded as an accident scenario.

2. Thermal analysis

2.1. Analyzed smartphone model

For the observation of thermal behavior during various operation states of the smartphone, following major components and their arrangement considered as shown in Fig. 1. The size of device body is 153.5 × 73.9 × 7.9 mm, which is a typical dimension of the smartphone device. Two graphite sheets (150.0 × 70.0 mm) are placed near the front glass and backplate for the efficient heat dissipation utilizing their high thermal conductivity and small

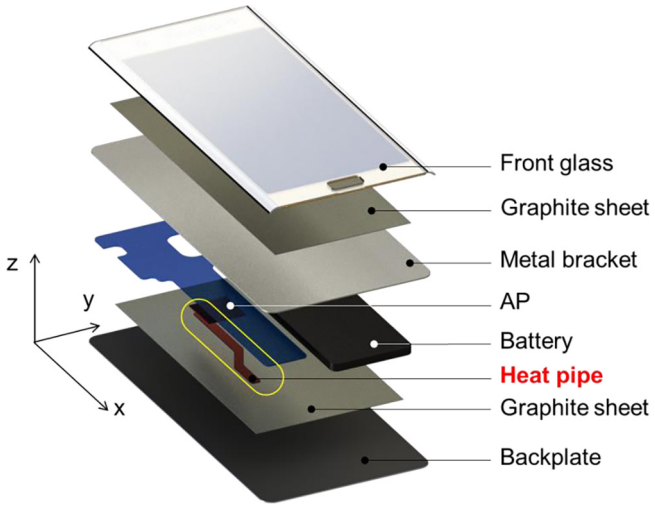

Fig. 1. Teardown structure of analyzed smartphone model by MARS and CFD simulations.

weight. They spread thermal energy generated from the AP or other heat-generating components in a short time. Below the graphite sheet at front side, metal bracket having same dimension with graphite sheet was installed to protect the electric components in printed circuit board (PCB). The AP located near the battery with gap of 2.0 mm to secure the volume for touch-pen embedment. In case of battery location, it was found adjacent to the PCB for the thinner design. In addition, the copper heat pipe, which delivers heat from the AP without external power source, was also considered in this study. The heat pipe, employing water as working fluid, was designed to have 0.4 mm thickness to minimize total thickness of the device and to maintain compact design. The center position of heat pipe, having 4.0 mm width and 100.0 mm length, was assumed to be located at below the AP (Both ends of heat pipe contacted to graphite sheet as heat sink). Water has a very high figure of merit, which is an indicator of heat transfer performance of heat pipe, due to high latent heat and surface tension in wide range of operating temperatures, compared to other heat transfer fluids such as refrigerants, heat transfer oils, and liquid metals. Therefore, water was selected as a working fluid of heat pipe in analyzed smartphone model in this study. Although thermal pad or thermal grease, which are widely used heat conduction material in mobile electronics, were not modeled in this analysis, the effect of contact resistances between the components were also neglected.

Thermal properties and thicknesses of the components [1] considered in the thermal analysis are summarized in Table 1. The thermal conductivities and volumetric heat capacities of the components were assumed to be constant. Front glass in Fig. 1 includes the glassy material and display in Table 1, and AP is assumed to have equal thermal properties with those of PCB. In addition, shields located at front and back of the PCB.

2.2. Analysis conditions

Heat generation rate of the components in the device was selected as input parameter to deduce the scenario resulting in smartphone explosion in terms of thermal management with observation on the thermal management capacity of current smartphone model. The LIB in the analyzed smartphone was assumed to have a discharge capacity and voltage of 3500 mAh and 3.85 V, respectively, as presented in Table 2. The thermal design power of AP (Snapdragon 820 or Exynos 8890) is 4 W with a maximum power consumption of 8 W required to operate the quadcore. The C-rate is a measure of rate at which a battery is charged or discharged relative to its maximum capacity. Thus, the operating current is 2.08 A corresponding to a discharge rate of 0.6 C and maximum heat generation from the AP is 4 W. Therefore, overcurrent (1 C), maximum operation, and normal operation of functionality of the AP (0.4 C and 0.6 C) were selected as the scenarios for analysis.

The discharge constant current and constant voltage conditions were assumed for all the analyzed cases. Additionally, heat generations of the battery were considered. The heat generation from LIBs can be divided into Joule heat and reaction heat as shown in Eq. (1). Joule heat is generated by overpotential and current, where voltage drops due to internal resistance. Open circuit voltage, V_{OCV}, varies with state of charge (SOC) and temperature because the internal resistance is a function of various factors such as SOC, temperature, and aging. The operating current, I, and effective entropic potential determine the reaction heat [22–24]. The operating current is controlled by the discharge rate, which is proportional to power consumption. The effective entropic potential, $T(\partial V_{OCV,SOC}/\partial T)$, also varies with the parameters that affect the open circuit voltage.

Table 1
Thermal Properties and Thicknesses of the Components in Analyzed Smartphone.

Components	Thickness [mm]	Thermal conductivity [W/mK]	Heat capacity [$\times 10^6$ J/m^3 K]
Glassy material	1.0	1.0	1.830
Backplate metal	0.25	10.0	1.350
Graphite sheet	0.025	10.0	1.520
PCB	0.8	1.0	1.332
Shields	0.15	15.0	3.640
Metal bracket	0.275	15.0	3.640
Display lumped	2.0	0.1	1.200
Heat pipe (copper)	0.4	385	3.4944
Battery	4.0	1.0	2.1930

Table 2
Detail specification of modeled LIB.

Parameters	Specifications
Anode material	Graphite
Cathode material	$LiFePO_4$
Nominal current	3500 mAh
Nominal current	3.85 V
Nominal capacity	13.475 Wh

$$\dot{Q} = \dot{Q}_{Joule} + \dot{Q}_{rea} = I(U_{SOC,I} - U_{OCV}) - IT\left(\frac{\partial U_{OCV,SOC}}{\partial T}\right) \quad (1)$$

The heat generation in the battery is inversely proportional to SOC and proportional to the discharge rate [25–27]. In addition, heat generation of the battery during charge and discharge depends aging of battery, materials of cathode and anode, normal capacity, and other various parameters. Coupling of many parameters on battery heat generation provides difficulty in the prediction. The heat generation from the LIB is generally varies from 5% to 60% of the discharge capacity [25–27]. Therefore, the discharge rate (30.3% of power dissipation) of LIB [26] with a graphite anode in analyzed smartphone model was assumed for a conservative estimate of the heat generation. The heat generated from AP and battery was modeled as constant volumetric heat sources for the corresponding solid domains. Thus, total four cases were simulated as presented in Table 3 using commercial computational fluid dynamics (CFD) code, ANSYS CFX, and multidimensional analysis for reactor safety (MARS) code which was developed by Korea Atomic Energy Research Institute to analyze the thermal-hydraulic phenomena in nuclear reactors.

2.3. Analysis method

The MARS code is a one-dimensional transient code that calculates the mass, momentum, and energy conservation for a two-phase flow [28]. The heat conduction module is also included in the code to solve the heat transfer in two-dimensional solids. The governing equation (Eq. (2)) and boundary condition (Eq. (3)) for the heat conduction module are as follows:

$$\iiint_V \rho(T,x)\frac{\partial T}{\partial x}\left(\bar{x},t\right)dV = \iint_S k\left(T,\bar{x}\right)\bar{\nabla}T\left(\bar{x},t\right)\cdot d\bar{s} + \iiint_V S\left(\bar{x},t\right)dV \quad (2)$$

$$h(T(t) - T_{sk}(t)) + k\frac{\partial T(t)}{\partial n} = 0 \quad (3)$$

The previously mentioned accident scenarios for the target device were simulated utilizing the heat conduction and convection modules. The convection module was activated to analyze heat transfer at the interface between the atmosphere and case material and inside the heat pipe, which is also called the thermal spreader. The main components of analyzed smartphone model used in MARS and CFD analyses are shown in Fig. 1. Two graphite sheets near the front glass and backplate are placed on the smartphone model for their high thermal conductivity, small weight, and thin design. They spread thermal energy generated from the AP or other heat-generating components in a short time. The heat pipe in the smartphone model delivers heat from the AP without external power source, as per its working principle. An ultra-thin mesh metal wicked heat pipe of 0.4 mm thickness was applied to the analyzed smartphone model to minimize its volume as it is important to reduce total thickness of the device and to maintain compact design. Heat transfers in x- and z-directions were modeled in the simulation performed for MARS.

Three-dimensional heat transfer was calculated by ANSYS CFX. Dimensions and thermal properties of the components utilized in the analyses are referred from Gurrum et al. (2012) [1]. Heat pipe was modeled as a solid domain having effective thermal conductivity, which is converted value from the thermal resistance of conventional copper heat pipe [29]. Heat transfer between all connected components are as boundary condition of conservative heat flux interface condition. The governing equation (Eq. (4)) for the energy conservation of all domains is as follows [30].

Table 3
Specified conditions for thermal analyses of smartphone.

Case number	Discharge rate (C)	AP heat generation (W)	Battery heat generation (W)	Remarks
#1	0.6	4.0	0.0	Operation state with maximum power consumption of AP (neglect the heat generation from battery)
#2	0.4	1.4	1.64	Operation state with normal power consumption of AP (consider the heat generation from battery)
#3	0.6	4.0	2.45	Operation state with maximum power consumption of AP (consider the heat generation from battery)
#4	1.0	9.5	4.08	Operation state with overcurrent (consider the heat generation from battery)

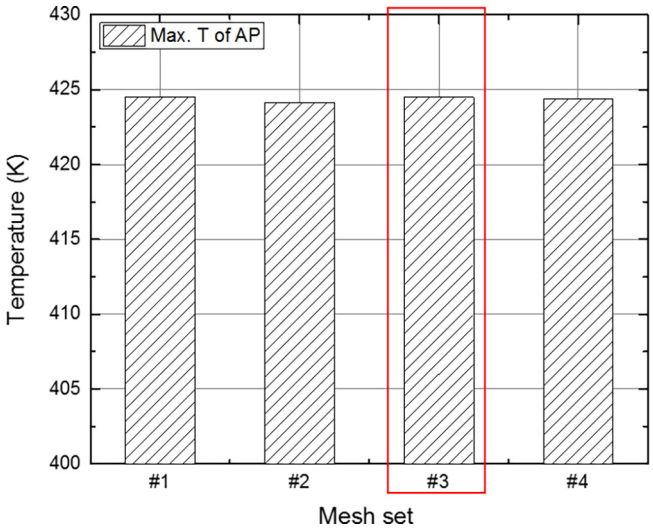

Fig. 2. Grid dependency test (ANSYS-CFX).

$$\frac{\partial(\rho h)}{\partial t} - \nabla \cdot (k \nabla T) = S_E \tag{4}$$

In the CFD simulation, convective boundary condition was set as heat transfer coefficient of 10 W/m^2 K, which was deduced by sensitivity study by comparison with MARS analysis results utilizing boundary condition as air convection. Interfaces between the components were connected as general grid interfaces for exchange of thermal energy [30] Total elements in the grid model were 25 M tetrahedra mesh, where current set, #3 was chosen from grid independency test. Comparison of maximum temperature of AP of various size of grid sets are in Fig. 2. In fact, it was found that several number of layers of thin graphite or display panel are required, rather than average size of elements, such that minimum 3 layers of elements are constructed for all components in simulation in this study.

In both code simulations, initial temperatures of the components and the environment were assumed as room temperature. The walls, except front and back plates, were set to an adiabatic condition to imply a water-and-dustproof design. The simulations were maintained until steady state or until the thermal runaway temperature (65 °C [22–25]). The three-dimensional simulation can analyze the local thermal behaviors in detail, while 1D simulation has advantage of transient calculation, compared to 3D simulation with equal computational resource. Transient calculation can provide the information on sequences of thermal behavior. In addition, verification of analyses results can be conducted by comparison of calculation results, obtained from both codes.

3. Results and discussion

3.1. Temperature behaviors at various power consumptions

Simulation results focused on temperatures of the components because those are representative output parameter indicating the thermal management performance of the device. Table 4 summarizes the average temperatures for AP, battery, and surface (front glass) under specified conditions. Both codes showed good agreement with each other. The deviations in temperature predictions in MARS and ANSYS-CFX were due to the 3-D heat conduction of each component. It is noteworthy that temperature calculated by MARS, which is calculated in 1D nodalization, can give transient trends of temperature increase thus saving computational resources. From the comparison of cases #1 and #3, it is evident that internal heat generation of the battery has significant effects on temperature evolutions of the components, that is case #3 shows higher temperatures by 12 °C compared to case #1. Therefore, the self-heating of battery was considered for analysis of discharge rate effect.

Temperature evolutions according to the cases are plotted in Fig. 3. Fig. 3 shows that temperature in the AP increases sharply in the initial phase of heat dissipation due to relatively high heat flux. After reaching the certain temperature points, temperature increases are dominated by heat conduction (thermal conductivities of the components). At the time that heat pipe temperature reaches operating temperatures (60–70 °C), rate of increase in temperature was reduced as shown in Fig. 3b and c. However, the effect of heat pipe is insignificant to perfectly dissipate the heat. Therefore, the temperature increase rates were recovered. In overcurrent case (case #4), the rate of temperature increases at AP and PCB differ from those of battery and surface despite their thickness are very thin. The generated heat from the AP and battery were conducted to other components by the graphite sheets resulting in an increase in their temperatures.

Temperature distributions at steady states for each case were analyzed by ANSYS CFX code and they are plotted in Fig. 4. As shown in Fig. 4a–c, the maximum temperature of the AP was near

Table 4
Simulation results of MARS and ANSYS CFX according to specified conditions.

Case number	Analysis code	Avg. surface temperature (°C)	Avg. AP temperature (°C)	Avg. battery temperature (°C)
#1	MARS	43.81	57.95	46.11
	ANSYS CFX	41.66	56.16	42.46
#2	MARS	35.1	42.73	36.53
	ANSYS CFX	37.76	43.06	38.46
#3	MARS	54.49	69.54	57.29
	ANSYS CFX	52.66	67.36	53.96
#4	MARS	74.47	127.5	79.17
	ANSYS CFX	82.96	117.26	85.46

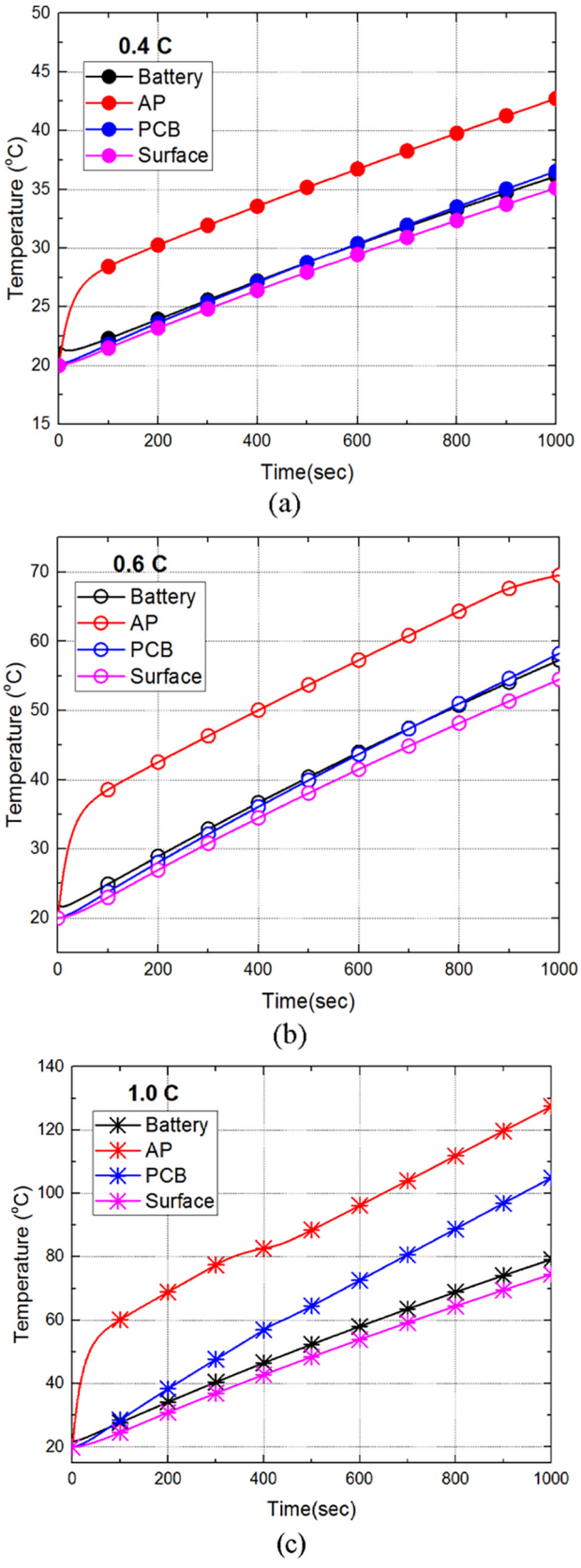

Fig. 3. Temperature evolution results of MARS code according to specified conditions (a) case #2, (b) case #3, (c) case #4.

the pen case in all the simulated conditions. In addition, the maximum temperature in the battery was near the AP in all the simulated conditions because of heat conducted by the graphite sheet

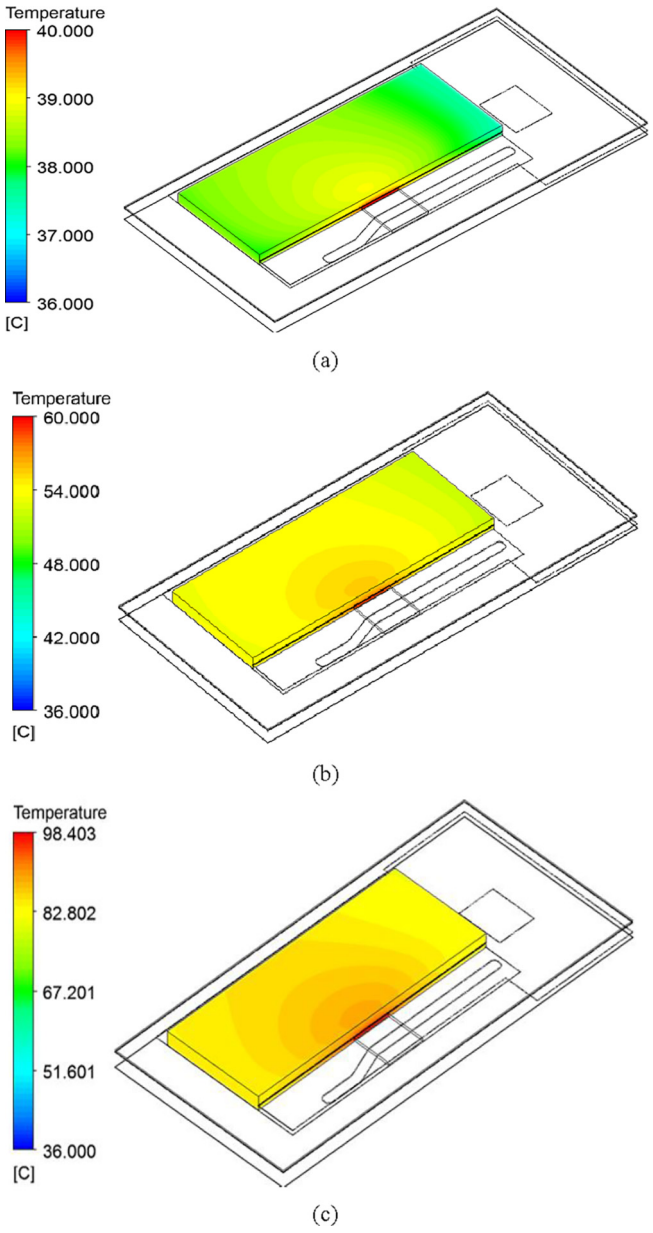

Fig. 4. Analyzed temperature distributions of target device according to specified conditions (a) case #2, (b) case #3, (c) case #4.

from AP to the battery. The battery temperature was found to increase even under small amounts of heat. The simulation for operation with maximum power consumption of the AP showed that temperatures of all the components were lower than their thermal limits (80 °C for AP [1–4] and 60 °C for battery [22–25]). However, the safety margin was insignificant.

The over-current condition (Fig. 3c) shows that maximum temperature of the battery was 98.56 °C, which was much higher than the temperature limit of 65 °C for lithium-ion batteries. This implies that the battery may explode due to high temperature when the AP consumes power higher than the designed value, which can frequently occur due to watching YouTube, playing mobile games, or running other high-load applications. In addition, if the smartphone device added function such as iris scanner, which requires instant high-power consumption in the AP, the occurrence possibility of overcurrent could be extended. Therefore, one possible cause for the battery explosion is overcurrent in the circuit through high power dissipation due to the iris scanner. It

is a logical guess because battery explosions have not been reported in other smartphone models, which do not have functionalities requiring high power consumption such as iris scanner, although they have batteries of equally high capacity.

3.2. Limitation of heat pipe

Heat pipes have been introduced in recent smartphone models for their efficient and passive heat dissipation properties. This was expected to solve the problem with heat dissipation in smartphones. However, the heat pipe could not spread the heat, generated by the AP over a wide area, efficiently in analyzed smartphone model. Because the heat pipe is very thin (0.4 mm), heat conduction near the AP is faster than in lateral directions on the graphite sheet, where it has a relatively lower temperature as shown in Fig. 4. This implies that thermal energy may affect the battery temperature evolution directly. Although heat pipe was designed to spread heat quickly to a low temperature region, it appears that functionality of the heat pipe failed partially due to its thin structure and its placement with respect to the AP and battery of analyzed smartphone. The MARS analysis results on heat transfer rates of the heat pipe under the postulated operating conditions are plotted in Fig. 5.

The heat pipe started to operate, as the temperature of working fluid reach the saturation temperature corresponding to the operating pressure (50 °C, because the operating pressure of the heat pipe embedded in the analyzed smartphone was assumed as 0.2 bar). The onset of operation coincided to the initiation of vaporization of the working fluid as shown in Figs. 5 and 6. The heat transfer rate through the heat pipe was increased as the AP temperature increased, owing to improved convection and vaporization of the working fluid with increase of temperature difference between heat source and sink. The heat pipe transferred about 15% of heat generated from the AP in cases of #2 and #3. However, the vapor temperature inside the heat pipe was increased continuously when the device operated with overcurrent (case #4) as shown in Fig. 6. The continuous increase of vapor temperature resulted from the limited heat transfer capacity of the heat pipe owing to dry-out. The low heat transfer capacity of the heat pipe is expected behavior based on operating temperature of the heat pipe. The heat pipe implemented in smartphones must operate at low temperatures to maintain the AP temperature below the

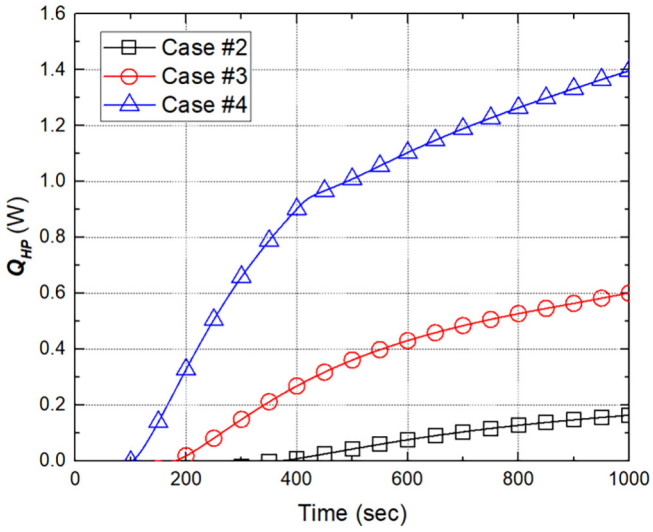

Fig. 5. Variations of heat transfer rates through heat pipe according to operating conditions of smartphone.

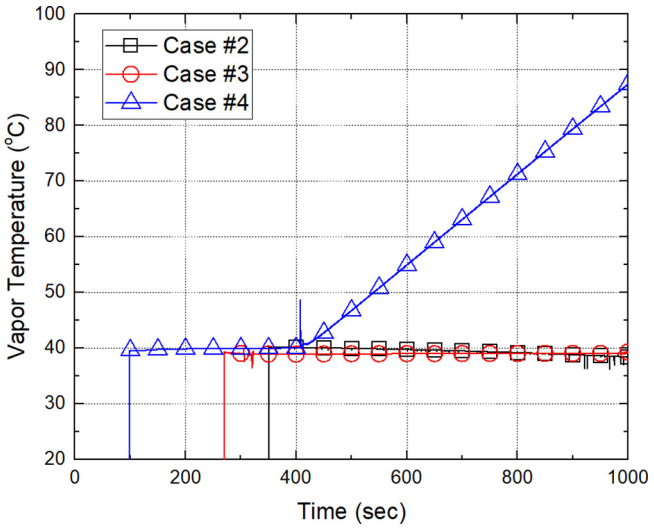

Fig. 6. Variations of vapor temperatures inside heat pipe according to operating conditions of smartphone.

specified temperature limit. The heat pipe should contain a vacuum to achieve low boiling temperature of its liquid. The volume of vapor created by boiling of the liquid is very large at subatmospheric pressures. Thus, it dries out the inner wall of the heat pipe. The maximum heat transfer rate of the heat pipe was confirmed as 0.9 W, which showed the slope change in heat transfer as shown in Fig. 4. After the heat pipe reached its operation limit, the heat transfer through the heat pipe was achieved in a manner of conduction through the metal container. From the analysis results, it was deduced that the heat pipe embedded in the smartphone has limited heat transfer capacity owing to its miniaturization and low operating temperature condition.

3.3. Effects of heat sink and inclination

Temperature of the heat sink is an important parameter that determines heat transfer rate of the heat pipe. From the perspective of heat transfer, most smartphones use an ultimate heat sink in the form of air convection from the display and backplate. This device design offers the heat pipe limited access to the ultimate heat sink and heat sink temperature affects the cooling performance of the smartphone. Additionally, the heat pipe, which was analyzed in the previous section, operated in vertical direction. Therefore, the heat transfer rate through the heat pipe would be reduced when the smartphone operates in horizontal or anti-gravity direction owing to reduction of driving force (gravitational force) in convection of working fluid. Therefore, the effects of heat sink temperature and inclination of the device on thermal management strategy using heat pipe were evaluated. The heat sink (atmosphere) temperature was varied 25–35 °C with 5 °C gap, and inclination angle of the smartphone was varied 0, 45, and 90° for each heat sink temperature. The smartphone model was assumed to be operated with maximum power consumption. All the cases were analyzed by MARS code, which was verified by comparison with analysis results of ANSYS CFX.

The temperature distributions at steady states according to operating conditions are compared as shown in Fig. 7. The temperatures of AP and battery were increased as the heat sink temperature increased. The reduction of inclination angle of smartphone further increased the component temperatures compared to vertical direction, because the heat transfer rate of the heat pipe was reduced, because the convection of liquid assisted by gravity was decreased. Reduction of driving force for working fluid convection

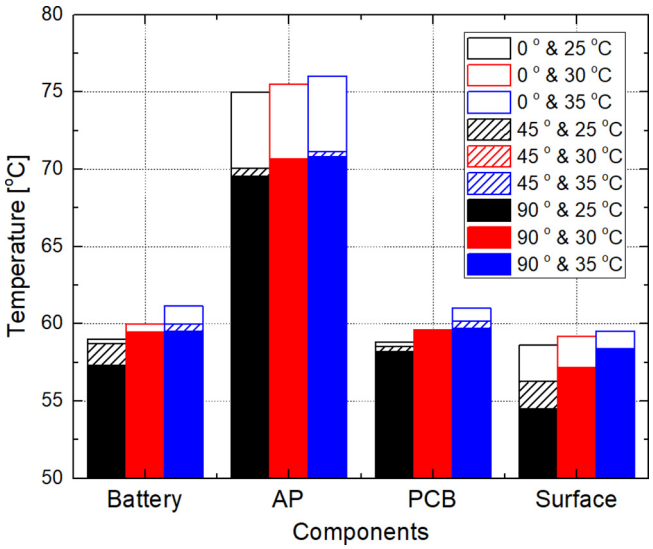

Fig. 7. Temperatures of components at steady states according to heat sink temperatures and inclination angles.

inside the heat pipe and conservative heat sink temperature sufficiently affect the component temperatures. Additionally, the effect of inclination angle, which dominates the coolability of heat pipe, was higher than heat sink temperature, indicating the embedded heat pipe significantly manage the heat inside the smartphone. Despite the temperatures of the components were below the temperature limits (80 °C for AP and 65 °C for battery), the thermal margins are insufficient to guarantee the integrity, because there are unpredictable elements influencing on the cooling capacity. Hence, the conservatism on the boundary conditions regarding the heat pipe performance and cooling capacity of the device must be considered in thermal design of smartphone.

In summary, the margin of safety in analyzed smartphone at maximum operation appears to be low owing to its compactness including space reserved for touch-pen, waterproof and dustproof design, internal heat generation of the LIB, and possibility of overcurrent arising from additions to AP functionalities as shown in Fig. 8. The implementation of functionality demanding high power consumption in AP could lead the overcurrent in the circuit. The overcurrent can easily heat the battery because internal heat generation is a crucial factor affecting thermal energy dissipation in smartphones with rise in energy density of the battery. Thus, multiple barriers preventing or mitigating the overcurrent must be fulfilled in design stage of the mobile electronics. In terms of thermal management strategy, although heat pipes were installed on smartphones to dissipate the heat efficiently, its performance strongly depended on the operation direction and heat sink temperature. Additionally, the limited heat transfer capacity of the heat pipe due to the operating conditions and excess miniaturization was also confirmed from the simulation results. Therefore, design optimization with understanding on the hydrodynamic characteristics inside the heat pipe is recommended to utilize the heat pipe efficiently as a thermal management device in smartphones. To satisfy the recommendations on the thermal management in mobile electronics, especially for smartphone, safety analysis must be conducted in terms of deterministic and probabilistic safety assessments considering various parameters such as internal heat generation of battery, absence of heat sink, and efficiency of thermal management devices and strategies.

4. Conclusions

Competitive addition of functionalities in mobile electronics required higher energy density in their compact arrangements. Recently, smartphone explosions were occurred, though various cooling strategies have been studied and equipped to maintain their safety and appropriate operation. Although there are many possible scenarios resulting in the smartphone explosion, the failure of thermal management in the device has not been sufficiently highlighted as a main issue. Therefore, thermal management of smartphone model was analyzed profoundly in this study using MARS and ANSYS CFX codes to deduce the scenario, which could cause smartphone explosion, with observation of limited capacity of existing cooling strategies and effect of component arrangement on thermal management. Internal heat generation of LIB was postulated with overcurrent scenario which could be caused by addition of special functionality in AP. As a result, following remarks are obtained, and these findings must be considered in future analyses and design of electronic devices in terms of thermal management.

(1) Consideration about internal heat generation of LIB has significant effect on thermal analysis of smartphone. Both codes showed good agreement with their results each other for all cases.

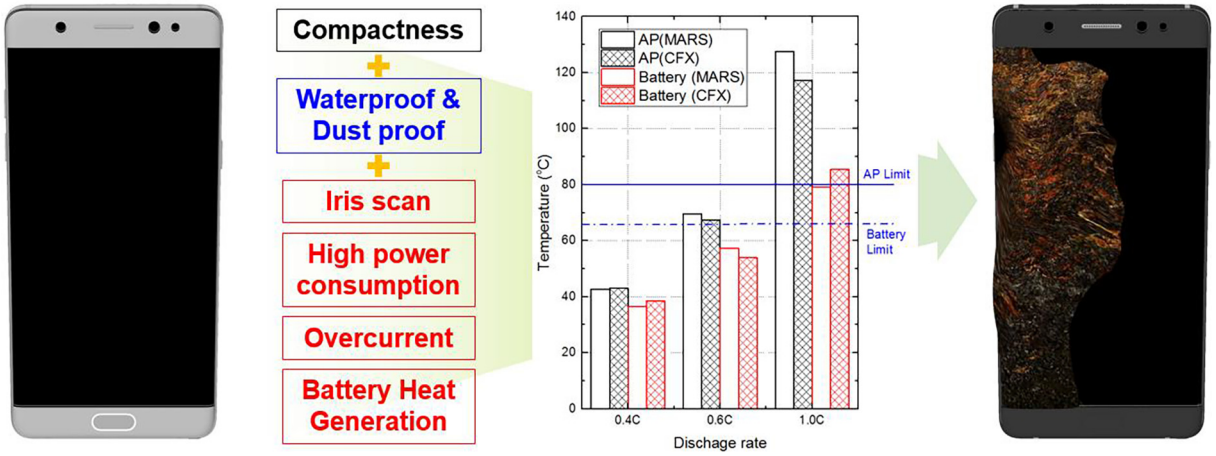

Fig. 8. Summary of smartphone explosion process using MARS and ANSYS CFX analysis.

(2) Arrangement of AP and battery is an important design criterion in terms of heat spreading, because heat focusing could be occurred according to their arrangement, increasing the local temperature.
(3) Temperatures of the components for the cases of normal and maximum operations of AP were lower than their thermal limits, however the safety margin is not significant.
(4) Overcurrent scenario through use of many functions in AP could cause thermal excursion of the device exceeding thermal limits of the components.
(5) Heat pipe was not an ultimate solution to remove the heat generation of AP due to its limited dimensions and operating conditions.
(6) Heat sink condition and inclination of the smartphone had significant effect on cooling capacity of the smartphone utilizing the heat pipe as a thermal management strategy.
(7) Ultimate cooling strategies must be developed to use safe and "smart" mobile electronics

Conflict of interest

None declare.

Acknowledgement

This research was supported by Basic Science Research Program and Nuclear Energy Program through National Research Foundation of Korea (NRF) funded by Korea government (MSIT) (2017R1A2B2008031), Human Resources Development of the Korea Institute of Energy Technology Evaluation and Planning (KETEP) grant funded by the Korea Government Ministry of Trade Industry and Energy (MOTIE) (No. 20174030201430), and Korea Hydro & Nuclear Power company through the project "Nuclear Innovation Center for Haeorum Alliance".

References

[1] S.P. Gurrum, D.R. Edwards, T.M. Golder, J. Akiyama, S. Yokoya, J.F. Drouard, F. Dahan, Generic thermal analysis for phone and tablet systems, in: Proceedings of Electronic Components and Technology Conference, IEEE, San Diego, CA, 2013, pp. 1488–1492.
[2] Q. Xie, M.J. Dousti, M. Pedram, Therminator: a thermal simulator for smartphones producing accurate chip and skin temperature maps, in: Proceedings of the 2014 International Symposium on Low Power Electronics and Design, La Jolla, California, CA, 2014, pp. 117–122.
[3] Z. Luo, H. Cho, X. Luo, K. Cho, System thermal analysis for mobile phone, Appl. Therm. Eng. 28 (14–15) (2008) 1889–1895.
[4] M. Pedram, S. Nazarian, Thermal modeling, analysis, and management in VLSI circuits: principles and methods, Proc. IEEE 94 (2006) 1487–1501.
[5] M.N. Sabry, Compact thermal models for electronic systems, IEEE Trans. Compon. Packag. Technol. 26 (2003) 179–185.
[6] M. Grimes, E. Walsh, P. Walsh, Active cooling of a mobile phone handset, Appl. Therm. Eng. 30 (2010) 2363–2369.
[7] V. Egan, J. Stafford, P. Walsh, E. Walsh, R. Grimes, An experimental study on the performance of miniature heat sinks for forced convection air cooling, in: 2008 11th Intersociety Conference on Thermal and Thermomechanical Phenomena in Electronic Systems, IEEE, Orlando, FL, May 28–31, 2008, pp. 497–509.
[8] V. Egan, P.A. Walsh, E. Walsh, R. Grimes, Thermal analysis of miniature low profile heat sinks with and without fins, J. Electron. Packag. 131 (3) (2009). 031004-1.
[9] E. Walsh, R. Grimes, Low profile fan and heat sink thermal management solution for portable applications, Int. J. Thermal Sci. 46 (11) (2007) 1182–1190.
[10] C.P. Tso, F.L. Tan, J. Jony, Transient and cyclic effects on a PCM-cooled mobile device, Therm. Sci. 19 (2015) 1723–1731.
[11] M. Jaworski, Thermal performance of heat spreader for electronics cooling with incorporated phase change material, Appl. Therm. Eng. 35 (2012) 212–219.
[12] Y. Tomizawa, K. Sasaki, A. Kuroda, R. Takeda, Y. Kaito, Experimental and numerical study on phase change material (PCM) for thermal management of mobile devices, Appl. Therm. Eng. 98 (2016) 320–329.
[13] Z. Ling, Z. Zhang, G. Shi, X. Fang, L. Wang, X. Gao, Y. Fang, T. Xu, S. Wang, X. Liu, Review on thermal management systems using phase change materials for electronic components, Li-ion batteries and photovoltaic modules, Renewable Sustain. Energy Rev. 31 (2014) 427–438.
[14] G. Zhou, J. Li, L. Lv, An ultra-thin miniature loop heat pipe cooler for mobile electronics, Appl. Therm. Eng. 109 (2016) 514–523.
[15] L. Lv, J. Li, Effect of charging ratio on thermal performance of a miniaturized two-phase super-heat-spreader, Int. J. Heat Mass Transf. 104 (2017) 489–492.
[16] Y.F. Maydanik, V.G. Pastukhov, M.A. Chernysheva, Development and investigation of a miniature copper-acetone loop heat pipe with a flat evaporator, J. Electron. Cooling Thermal Control 5 (2015) 77–88.
[17] X. Chen, H. Ye, X. Fan, T. Ren, G. Zhang, A review of small heat pipes for electronics, Appl. Therm. Eng. 96 (2016) 1–17.
[18] H. Aoki, M. Ikeda, Y. Kimura, Ultra thin heat pipe and its application, International 10th Heat Pipe Symposium, Taipei, Taiwan, Nov. 6-9, 2011, pp. 35–40.
[19] N.H. Naqiuddin, L.H. Saw, M.C. Yew, F. Yusof, T.C. Ng, M.K. Yew, Overview of micro-channel design for high heat flux application, Renewable Sustain. Energy Rev. 82 (2018) 901–914.
[20] Y. Ye, Y. Shi, L.H. Saw, A.A.O. Tay, Performance assessment and optimization of a heat pipe thermal management system for fast charging lithium ion battery packs, Int. J. Heat Mass Transf. 92 (2016) 893–903.
[21] S. Panchal, S. Mathewson, R. Fraser, R. Culham, M. Fowler, Experimental measurement of thermal characteristics of LiFeO4 battery, SAE Technical Paper, 2015-01-1889.
[22] P. Huang, Q. Wang, K. Li, P. Ping, J. Sun, The combustion behavior of large scale lithium titanate battery, Sci. Rep. 5 (2015) 7788.
[23] X. Feng, M. Fang, X. He, M. Ouyang, L. Lu, H. Wang, M. Zhang, Thermal runaway features of large format prismatic lithium ion battery using extended volume accelerating rate calorimetry, J. Power Sources 255 (2014) 294–301.
[24] X. Liu, Z. Wu, S.I. Stoliarov, M. Denlinger, A. Masias, K. Snyder, Heat release during thermally-induced failure of a lithium ion battery: Impact of cathode composition, Fire Saf. J. 85 (2016) 10–22.
[25] S. Wang, Entropy and heat generation of lithium cells/batteries, Chin. Phys. B 25 (2016) 010509.
[26] G. Liu, M. Ouyang, L. Lu, J. Ji, X. Han, Analysis of the heat generation of lithium-ion battery during charging and discharging considering different influencing factors, J. Therm. Anal. Calorim. 116 (2014) 1001–1010.
[27] J. Sun, G. Wei, L. Pei, R. Lu, K. Song, C. Wu, C. Zhu, Online internal temperature estimation for lithium-ion batteries based on Kalman filter, Energies 8 (2015) 4400–4415.
[28] B.D. Chung et al., MARS Code Manual, KAERI/TR-2812/2004, Korea Atomic Energy Research Institute.
[29] D.A. Reay, P.A. Kew, Heat Pipes, Elsevier, New York, 2006.
[30] ANSYS Inc., ANSYS, CFX-Solver Theory Guide, 2013.